

Metal supported and metal ion exchanged catalysts from palygorskite for acetylation reaction

Dhanya Balan A P & Pushpaletha P*

Department of Chemistry, Govt. College Kasaragod,
Kannur University, Kerala, India

Email: ppletha@rediffmail.com

Efficient solid acid catalysts from palygorskite have been developed by three modification methods, viz., acid activation, metal salt support (with FeCl_3 , MnCl_2 , CoCl_2 , SnCl_2 , ZnCl_2 and AlCl_3) and metal ion exchange (exchange with Fe^{3+} , Mn^{2+} , Co^{2+} , Sn^{2+} , Zn^{2+} and Al^{3+}) for acetylation reaction in the liquid phase. The prepared catalysts are characterized by XRD, SEM, FTIR, NH_3 -TPD, cation exchange capacity, and BET surface area, and their catalytic activity tested by acetylation of primary and secondary alcohols using acetic acid. The modified palygorskites are found to be efficient catalysts for acetylation of alcohols with no loss of catalytic activity even after four cycles. The iron exchanged palygorskite is found to be most active.

Keywords: Catalysts, Supported catalysts, Solid catalysts, Cation exchange capacity, Acid activation, Acetylation, Palygorskite, Acetic acid, Alcohols

Acetylation of alcohol is one of the most important synthesis methods and finds applications in industries dealing in food and cosmetics, fragrances, solvent plasticizers, pharmaceuticals, etc. It provides an efficient means for protecting OH group during construction of polyfunctional molecules such as carbohydrates, nucleosides, steroids, and natural products¹. The main advantages of using the acetyl group for protection is that it can be easily introduced, is stable in acidic reaction conditions, can be easily removed by mild alkaline hydrolysis².

Acetylation is commonly carried out by homogeneous catalysis with acetic anhydride in presence of bases^{1,3-5}, acids⁶⁻⁸, or metal triflates⁹⁻¹¹. However, these methods have several drawbacks, such as long reaction time, use of highly flammable and expensive reagents, formation of byproducts, low yield of desired product, difficulty in separation and recovery of desired product, disposal of spent catalyst, high corrosion, toxicity, etc.¹² In view of this, development of eco-friendly heterogeneous solid acid catalyst for acetylation reaction is of high importance.

Various solid acid catalysts are reported for acetylation reactions using acetic anhydride, viz., zeolites¹³⁻¹⁶, mesoporous supported Lewis and Bronsted acids¹⁷⁻²⁰, supported heteropoly acids on silica and silica-zirconia²¹ modified metal oxides, supported ionic liquids, Nafion or Nafion like composites²². However, most of these catalysts show several disadvantages such as rapid catalyst deactivation, low product yields, complexity in method of preparation, production of wasteful products and severe reaction conditions²³.

Acetic acid is generally preferred as the acetylating agent in the catalytic acylation of alcohols and phenols because water is the only byproduct. Modified palygorskite is reported to catalyse reactions such as oxidation of ethanol²⁴ and styrene²⁵, polymerization of caprolactone²⁶, synthesis of alcohol²⁷, etc. Acid activated palygorskite is reported to be an efficient solid acid catalyst for acetylation reaction²⁸. The acid activation improved the surface area and catalytic properties of the clays. In addition, acidity, surface area and pore size distribution of natural clay minerals can be controlled by metal salt support and metal ion exchange. Initial screening of various metal reagents supported on acid treated palygorskite revealed that there was a definite enhancement in activity of FeCl_3 supported palygorskite. In the case of metal ion exchanged clay minerals, the catalytic activity arises from the intrinsic activity of the metal ion and surface acidity generated due to cation exchange²⁹. The restricted environment of the clay interlayer often facilitates the shape selectivity of the reaction products. The acidity and polarisability of water in the environment can be varied by suitable choice of the cation in inter lamellar space.

To the best of our knowledge, the catalytic activity of the clay has not been explored so far. Herein, we have compared the catalytic potential of solid acid catalyst developed from natural palygorskite by different modification methods like acid activation, metal salt support and metal ion exchange with a view to develop a more efficient catalyst for the acetylation of alcohols by using acetic acid.

Experimental

Clay mineral used in the present study was procured from Korvi Fuller's Earth Ltd., Karnataka,

India. Other chemicals used, i.e., ferric chloride, stannous chloride, manganese chloride, zinc chloride, sodium hydroxide, hydrochloric acid, sulphuric acid, *n*-hexane, *n*-heptane, 2-butane, lauryl alcohol, etc., were obtained from Loba Chemie (AR grade).

To purify the clay, it was suspended in water, stirred vigorously and the coarser particles were allowed to settle. The carrier fines were passed through a 350# B.S sieve to separate the clay particles of size less than 45 μm . The slurry was dried and the dry mass was disintegrated

The first step in the preparation of the catalyst was the acid activation of the raw clay. Metal salt supported and metal ion exchanged catalysts were prepared from this acid activated catalyst.

For acid activation, the above raw clay sample was refluxed for 45 min with 0-2 N sulphuric acid solutions (1:4 ratio) in a 250 mL round bottom flask fitted with a condenser. It was then cooled and added to 1 L water and allowed to settle. After filtering and washing to remove any anions, the sample was dried in an air oven at 110 °C for 6 h. Catalysts prepared were designated as PS0 – PS5 (Table 1).

Metal salt supported palygorskite samples were prepared by treating the acid activated clay mineral (PS₂) with FeCl₃, MnCl₂, CoCl₂, SnCl₂, ZnCl₂ or AlCl₃ in acetonitrile solution and stirring the resulting solution for 3 h with a magnetic stirrer. The catalysts were then dried and activated at 110 °C and designated as given in Table 1.

The ion exchanged palygorskite samples were prepared by exchanging the acid activated clay mineral (PS₂) with Fe³⁺, Mn²⁺, Co²⁺, Sn²⁺, Zn²⁺ and Al³⁺ by treatment with the corresponding metal chlorides in aqueous solution. The resulting solution was stirred for 3 h with a magnetic stirrer, washed till free of chlorides, dried and activated at 110 °C. The ion exchanged catalysts are designated as given in Table 1.

X-ray diffraction (XRD) patterns were recorded on a Bruker D8 Advance X-ray diffractometer.

Morphological studies were carried out by scanning electron microscopy (JEOL, model JSM-6390LV). FTIR spectra were recorded on a Thermo Nicolet spectrometer in the range of 4000-400 cm^{-1} as KBr pellets. The dehydration and decomposition processes of the raw and acid treated palygorskite were studied by TG-DTA analysis. The surface area of the sample was measured by N₂ adsorption (Micromatrix, Gemini VII ver. 3.01) and calculated by the Brunauer-Emmett-Teller (BET) method. The acidity of the clays, containing both Bronsted and Lewis acid sites, was measured by sodium hydroxide titration and NH₃- TPD. Cation exchange capacity measurements were made by the ammonium absorption technique³⁰. The amounts of silicon, aluminium and iron present in the raw and acid treated palygorskite were obtained by chemical analysis of the clay minerals and are given as the corresponding oxides.

For studying the catalytic activity, reactions were carried out in an round bottom flask fitted with condenser. In a typical experiment, the reaction mixture comprising cyclohexanol and glacial acetic acid was refluxed in the presence of 0.5 g catalyst. After 3 h, the reaction was stopped and the catalyst was separated by filtration. The filtrate was washed with saturated sodium bicarbonate solution to make it acid free and dried over anhydrous sodium sulphate and analyzed by GC.

Results and discussion

X-ray diffraction patterns of the raw and acid activated sample indicate that the major mineral in the sample is palygorskite (Fig. 1). The peak at $2\theta = 8.5^\circ$ ($d = 10.30 \text{ \AA}$), is characteristic of palygorskite mineral, while the peaks at $2\theta = 19.84^\circ$ and 26.7° ($d = 4.4 \text{ \AA}$ and 3.3 \AA) indicate the presence of quartz as impurity. The sample was found to be reasonably pure except for traces of carbonate as impurity ($2\theta = 29.49^\circ$, $d = 3.02 \text{ \AA}$). Upon acid activation the carbonate impurity dissolves and hence the peak for carbonate impurity is not seen.

Table 1 – Catalysts prepared by acid activation, metal salt support and metal ion exchange methods

No.	Acid activated catalyst		Modified catalysts			
	H ₂ SO ₄ (N)	Support	Metal	Source	Metal salt supported catalyst	Metal ion exchanged catalyst
1	0	PS0	Fe	FeCl ₃	PS2Fe	PS2FeI
2	0.1	PS1	Mn	MnCl ₂ .4H ₂ O	PS2Mn	PS2MnI
3	0.5	PS2	Co	CoCl ₂ .6H ₂ O	PS2Co	PS2CoI
4	1.0	PS3	Sn	SnCl ₂ .2H ₂ O	PS2Sn	PS2SnI
5	1.5	PS4	Zn	ZnCl ₂	PS2Zn	PS2ZnI
6	2.0	PS5	Al	AlCl ₃ .6H ₂ O	PS2Al	PS2AlI

The SEM micrographs of the raw sample show elongated lath shaped crystals (1-3 μm length, diameter of the order of 0.1 μm) and their bundles, which is characteristic of palygorskite mineral (Fig. 2). The particles exist as aggregates and size of each aggregate ranges from 1–6 μm . The SEM

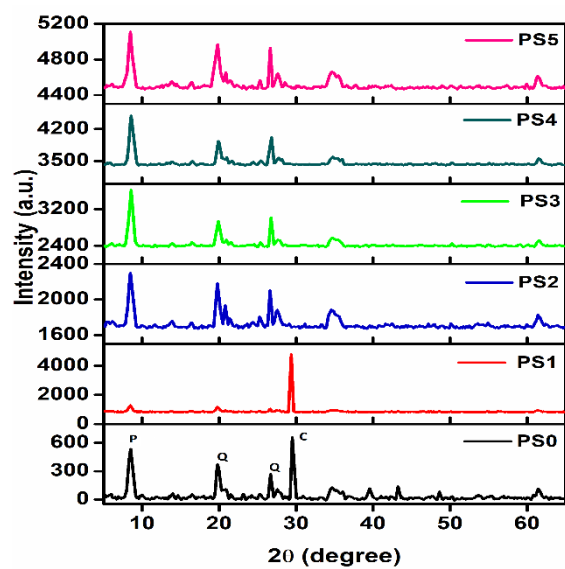


Fig. 1 – XRD patterns of raw and acid activated palygorskite samples.

images of the acid treated samples show that the acid treatment has not affected the fibrous morphology of palygorskite. It is reported that during acid activation, the tetrahedral layer in palygorskite tends to preserve its fibrous morphology³¹. Even after the removal of the octahedral layer during acid activation, the fibrous morphology is maintained, indicating the retention of order in the tetrahedral layer in palygorskite.

Differential thermal analysis shows that dehydration of palygorskite take place in a series of three steps. In the first two steps at 74.70 $^{\circ}\text{C}$, and 187.36 $^{\circ}\text{C}$, both hygroscopic and zeolitic water were lost (Supplementary data, Fig. S1). The third step occurred at 677.77 $^{\circ}\text{C}$, when water of coordination was lost. The entire dehydration step was endothermic. The partial dehydration of bound water is attributed to the difference in bonding position of water in the structure of these minerals and resulted in the formation of palygorskite anhydride. As the concentration of acid for activation was increased, the intensity of these steps decreased. Thus, only two steps are observed in the sample PS5 (2 N H_2SO_4). The first (up to 100 $^{\circ}\text{C}$) is the loss of water adsorbed by the free silica and the second, a very modest slope in the high temperature region of the TG curves, is

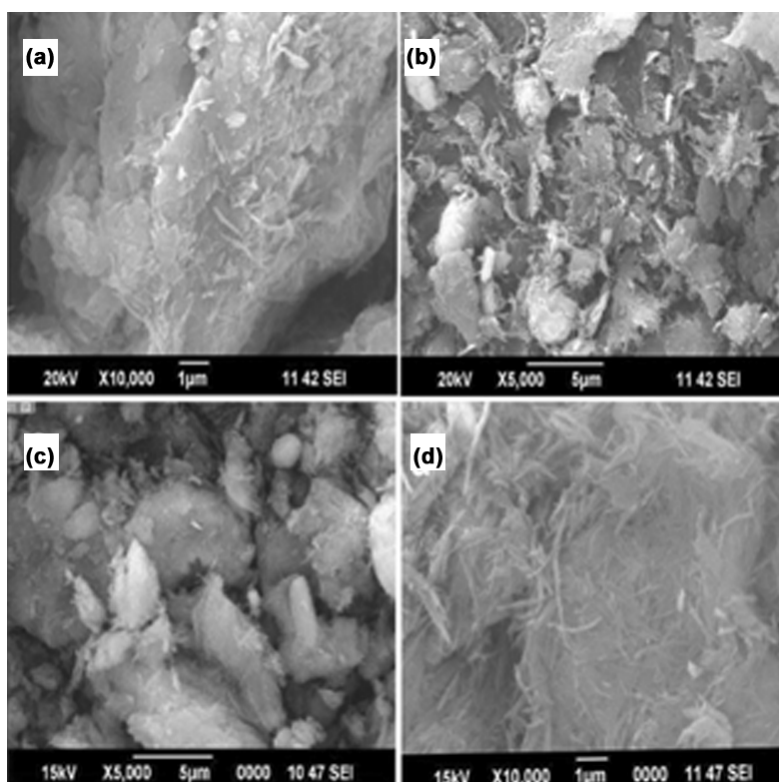


Fig. 2 – SEM images of raw palygorskite [(a) PS0 and (c) AM0], showing parallel bundles of fibrous palygorskite, and, acid activated palygorskite [(b) PS2 and (d) AM2], having a more porous structure, with the fibrous morphology maintained.

Table 2 – BET surface area and acidity of acid activated, metal salt supported and metal ion exchanged catalysts

Samples	BET surface area (m ² /g)	Pore volume (cm ³ /g)	Avg. pore dia. ^a (nm)	Surface acidity (meq./g)	CEC (meq./100 g)	Conv. (%)
PS0	146.34	0.043	1.675	162.64	47.71	59.88
PS1	156.04	0.045	1.675	193.63	59.64	68.33
PS2	159.04	0.047	1.671	200.30	71.50	75.00
PS3	169.10	0.049	1.675	191.74	53.67	66.19
PS4	192.48	0.055	1.687	169.49	49.70	65.00
PS5	210.57	0.060	1.686	184.90	41.74	64.20
PS2Fe	151.37	0.046	1.661	333.44	76.88	93.85
PS2Mn	75.26	0.047	1.602	281.63	73.82	76.79
PS2Co	92.08	0.059	1.617	273.42	64.74	75.37
PS2Sn	173.13	0.053	1.658	271.75	72.44	74.65
PS2Zn	125.35	0.080	1.627	266.75	70.86	68.81
PS2Al	137.59	0.029	1.768	265.46	69.32	67.34
PS2FeI	156.91	0.046	1.672	520.31	77.42	97.76
PS2MnI	-	-	-	461.72	74.32	82.91
PS2CoI	-	-	-	450.64	70.36	79.32
PS2SnI	-	-	-	446.52	72.77	81.43
PS2ZnI	-	-	-	440.36	71.83	80.35
PS2AlI	-	-	-	430.00	71.00	78.49

^aAvg. pore dia. = 4V/A by BET.

due to the elimination of silanol groups. This last step proceeds without important energetic effects (Supplementary data, Figs S2–S6).

FTIR of the raw clay sample showed sharp band at 3553 cm⁻¹, due to stretching vibrations of the OH bound to two Al³⁺ cation in the octahedral coordination (Supplementary data, Fig. S7). The bending vibrations of water appear as a strong band at 1657 cm⁻¹. The intensity of the Al-OH-Al band was found to decrease with the severity of acid treatment. Intense band at 1028 cm⁻¹ is due to the Si-O-Si stretching vibrations, which became broader on acid treatment indicating the gradual destruction of the crystal structure.

BET surface area, pore volume and average pore diameter of raw, acid activated, metal salt supported and metal ion exchanged palygorskite are given in Table 2. Surface area increased with the severity of acid treatment. While the raw sample had a surface of 146.3 m² g⁻¹, the maximum value of surface area obtained was 210.57 m² g⁻¹ for PS5. This increase in surface area with increase in acid concentration is due to the elimination of exchangeable cations and the consequent increase of SiO₂³².

The NH₃-TPD studies were carried out to evaluate the acid site distribution of the raw and acid activated palygorskite mineral (Fig. 3). Based on the desorption temperature maxima, the TPD profiles of raw and

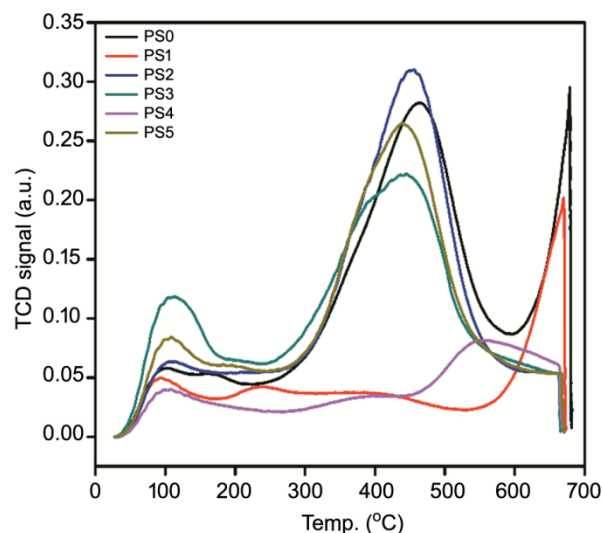


Fig. 3 – NH₃-TPD curves of raw and acid activated palygorskite catalysts.

acid activated palygorskite can be divided into three regions, corresponding to (a) intermediate or medium (100–200 °C), (b) strong (300–600 °C), and very strong acid strengths (>600 °C). Acid activated palygorskite exhibits three peaks at 100 °C, 410 °C and 650 °C, which can be correlated to three different types of active sites. The first and second peaks suggest that palygorskite possesses a large number of acid sites with intermediate and strong acid strength

respectively. PS2 shows higher activity, because the total acid sites of PS2 are greater than those of raw and other acid activated samples.

Surface acidity calculated by sodium hydroxide titrations is given in Table 2. Acidity of the raw sample is only 162.64 meq./g. On acid activation using 0.1 *N* H₂SO₄, acidity increased to 193.63 meq./g. The maximum value is shown by PS2, clay activated with 1 *N* H₂SO₄ (200.30 meq./g). The acidity increased initially with acid concentration, reached a maximum value and then decreased.

The physical properties of clay materials are dependent to a large extent on the exchangeable ions associated with the clay. Cation exchange capacity (CEC) of clays was determined by exchanging the cations of the clay by ammonium ions and measuring the amount of ammonium ions exchanged. Cation exchange capacity of raw and acid activated sample is given in Table 2. Cation exchange capacity of the raw sample is 47.71 meq./100 g. On acid activation, the CEC first increases and reaches a maximum and then decreases. Maximum cation exchange capacity was shown by the sample treated with 0.5 *N* H₂SO₄ (71.50 meq./100 g). With the severity of acid treatment, crystal structure starts collapsing and thus cation exchange capacity decreases.

SiO₂ in raw and acid treated palygorskite ranges from 53.40–61.56% (Supplementary data, Table S1). The amount of SiO₂ in palygorskite increases with the removal of aluminium, magnesium, iron, etc., during acid treatment. Silicon, which is the dominant constituent in the tetrahedral sheets of the clay, is relatively resistant to acid attack³³. The amount of aluminium and iron decreased with increasing acid concentration, which indicates that the ions Al³⁺ and Fe³⁺ were leached out during acid activation.

Catalytic activity of the raw and acid activated catalysts was studied for the acetylation of cyclohexanol using acetic acid. The PS2 sample (0.5 *N* H₂SO₄ treated sample) gave maximum conversion (Table 2). Catalytic activity of the PS2 catalysts was analyzed for both primary and secondary alcohols. The primary alcohols showed better conversions as compared to secondary alcohols (Supplementary data, Table S2). Catalytic activity of FeCl₃, MnCl₂, CoCl₂, SnCl₂, and ZnCl₂ supported catalysts was also monitored. Among the different metal supported catalysts prepared, the FeCl₃ supported catalysts gave maximum conversion (93.85%). This indicates that clay is not merely an

inert support, but exhibits selective synergistic effect on the activity of the metal cations it supports. In this context the presence of Fe in the clay seems to be a crucial factor.

Catalytic activity of Fe³⁺, Mn²⁺, Co²⁺, Sn²⁺, Zn²⁺ and Al³⁺ ion exchanged catalysts was also monitored for acetylation of cyclohexanol. Maximum conversion was obtained in the case of the iron-exchanged catalyst (97.76%). As shown in Table 2, among the various catalysts prepared by different modification methods, viz., acid activation, metal salt support and metal ion exchange, the metal ion exchanged catalyst are superior over all other catalysts. Catalytic activity of FeCl₃ supported and Fe³⁺ ion exchanged catalyst was also studied for both primary and secondary alcohols. As in the case of raw and acid activated catalysts, in this case also, the primary alcohols showed higher conversion than secondary alcohols (Table S2).

The effects of varying reaction time (1–4 h) and catalyst loading (0.25–1.00 g) on catalytic activity of iron exchanged catalyst were monitored for the acetylation of benzyl alcohol with glacial acetic acid. Maximum conversion was obtained in 3 h with a minimum of 0.5 g of iron exchanged catalyst for conversion of 0.05 mol alcohol. Reusability of the catalyst was also tested by using the same reaction. No reduction in percentage of conversion was observed even after four cycles. These results are given in Table S3 (Supplementary data).

Acidity, cation exchange capacity and the catalytic activity of the present catalysts were compared with catalyst prepared from the standard sample (AM) collected from Clay mineral Society of Attapulgate, Department of Geology, PFL1 US Repository, Missouri, Columbia. In our earlier experiments, PS2 (0.5 *N* H₂SO₄ treated sample) had shown the maximum activity. So the standard sample was also treated with 0.5 *N* H₂SO₄ (AM2). The acidity and cation exchange capacity values of acid activated sample AM2 (193.68 and 68.34), iron supported catalyst AM2Fe (340.34 and 75.30) and iron exchanged catalyst AM2FeI (540.36 and 78.97) were found to be comparable with those of the corresponding PS2 samples, PS2, PS2Fe and PS2FeI (Table S3). Catalytic activity of the AM samples was also comparable with the corresponding PS2 samples.

In conclusion, the present study showed that the major mineral present in the sample under study was palygorskite. Among the acid activated clay catalysts,

the 0.5 N H₂SO₄ treated clay mineral was found to be most active towards acetylation reaction. The catalytic activity was further improved by metal salt support and cation exchange modification. Activity of the metal salt supported catalyst was found to be in the order: FeCl₃ > MnCl₂ > CoCl₂ > SnCl₂ > ZnCl₂ > AlCl₃. The FeCl₃ supported catalyst showed the maximum acidity and CEC. Catalysts prepared by cation exchange were found to have better activity than the supported catalysts and the Fe³⁺ exchanged sample showed the highest activity (97.76%). The catalysts are found to be active towards acetylation of several primary and secondary alcohols. Reusability of the catalyst was excellent up to four cycles.

Supplementary data

Supplementary data associated with this article are available in the electronic form at [http://www.niscair.res.in/jinfo/ijca/IJCA_57A\(05\)649-654_SupplData.pdf](http://www.niscair.res.in/jinfo/ijca/IJCA_57A(05)649-654_SupplData.pdf).

Acknowledgement

The authors gratefully acknowledge the financial support provided by State Council for Science Technology and Environment under the “Back to Lab” Program.

References

- Green T & Wutz P, *J Med Chem*, 50 (2007) 1084.
- Heravi M, Behbahani F, Zadsirjan V & Oskooiee H, *J Braz Chem*, 17 (2006) 1045.
- Scriven E, *Chem Soc Rev*, 12 (1983) 129.
- Sano T, Ohashi K & Oriyama T, *Synthesis*, 1999 (1999) 1141.
- Vedejs E & Diver S T, *J Am Chem Soc*, 115 (1993) 3358.
- Chandrasekhar S, Ramachander T & Takhi M, *Tetrahedron Lett*, 39 (1998) 3263.
- De S, *Tetrahedron Lett*, 45 (2004) 2919.
- Iqbal J & Srivastva R, *J Org Chem*, 57 (1992) 2001.
- Saravanan P & Singh V, *Tetrahedron Lett*, 40 (1999) 2611.
- Chauhan K, Frost C, Love I & Waite D, *Synlett*, 1999 (1999) 1743.
- Ishihara K, Kubota M, Kurihara H & Yamamoto H, *J Am Chem Soc*, 117 (1995) 4413.
- Choudhary V, Patil K & Jana S, *J Chem Sci*, 116 (2004) 175.
- Derouane E, Crehan G, Dillon, C J, Bethell D, He H & Derouane-Abd Hamid S B, *J Catal*, 194 (2000) 410.
- Rohan D, Canaff C, Fromentin E & Guisnet M, *J Catal*, 177 (1998) 153.
- Freese U, Heinrich F & Roessner F, *Catal Today*, 49 (1999) 237.
- Smith K, Zhenhua Z & Hodgson P, *J Mol Catal A: Chem*, 134 (1998) 121.
- Gronnow M, Macquarrie D, Clark J & Ravenscroft P, *J Mol Catal A: Chem*, 231 (2005) 47.
- Yadav G & Pujari A, *Green Chem*, 1 (1999) 69.
- Yadav, G & Asthana N, *Ind Eng Chem Res*, 41 (2002) 5565.
- Yadav G & Krishnan M, *Chem Eng Sci*, 54 (1999) 4189.
- Bachiller-Baeza B & Anderson J, *J Catal*, 228 (2004) 225.
- Heidekum A, Harmer M & Hoelderich W, *J Catal*, 188 (1999) 230.
- Reddy B & Sreekanth, P, *Synthetic Comm*, 32 (2011) 2815.
- Wang K, Wang H, Pasupathi S, Linkov V, Shanji & Wang R, *Electrochim Acta*, 70 (2012) 394.
- Wang F, Zhang J, Liu C & Liu J, *Appl Clay Sci*, 105 (2015) 150.
- Wang G, Ma R, Chen T, Yan C, Gao J & Bao F, *Polymer Plastic Technol Eng*, 52 (2013) 1193.
- Guo H, Zhang H, Peng F, Yang H, Xiong L, Huang C, Wang C, Chen X & Ma L, *Appl Clay Sci*, 111 (2015) 83.
- Pushpaletta P & Lalithambika M, *Appl Clay Sci*, 51 (2010) 424.
- Sukumar R, Sabu K R, Bindu L V & Lalithambika M, *Stud Surf Sci Catal*, 113 (1998)
- Grimshaw R & Searle B, *Chemistry and Physics of Clays* (Western Printing Services Ltd, Bristol, Great Britain), 1960.
- Myriam M, Suarez M & Martin-Pozas J, *Clays Clay Miner*, 46 (1998) 225.
- Bouderiche L, Calvet R, Hamid B & Balard H, *Colloids Surf A: Physicochem Eng Aspects*, 392 (2011) 45.
- Xavier K, Santos M, Santhosh M, Oliveira M, Carvalho M, Osajima J & Filho E, *Mater Res*, 17 (2014) 3.